Progress In Electromagnetics Research M, Vol. 81, 203–213, 2019

Performance Comparison of Stepped and Smooth Dielectric Lens-Loaded Flat Reflectors

Veluchamy Lingasamy[1], Krishnasamy T. Selvan[1, *], and Patnam H. Rao[2]

Abstract—This paper presents the design of an X-band stepped lens-loaded flat reflector (STLR) using reflectarray unit cell approach. A flat reflector of size $15 \times 15\,\mathrm{cm}^2$, loaded with a 10×10 dielectric unit cell array, centre-fed by a horn antenna, is evaluated by simulation and measurement. The simulated performance of the proposed structure is compared with a smooth lens loaded plane reflector (SMLR) and microstrip reflectarray (RA), of equivalent cross section. The results are in good agreement for SMLR, whereas a fair match is observed only in the main lobes of RA. It is worth to note that the reported STLR has a reduced thickness compared to SMLR. Furthermore, a simulation-based study is carried out on the effect of tapering of the dielectric structure in the proposed design, and a similar performance to when stepping is used is noted.

1. INTRODUCTION

Reflector antennas are primarily used in space, radar, and remote sensing applications [1]. Conventional dielectric lens, artificial lens, and other dielectric loading techniques are also studied to enhance the gain of antennas such as horn, waveguide, and patch [2]. As an alternative approach, Barry et al. [3] proposed an antenna with shaped metal-backed dielectric, whose the thickness (and thus the depth of the shape) is varied to attain the required compensating reflection phase (delay) [3]. All these methods, in fact, involve phase compensation to the incident waves resulting in collimation [4, 5]. Kraus proposed a new antenna design called reflector-lens, by incorporating the principles of reflector and lens to attain a planar wavefront [6]. He theoretically illustrated that the thickness of dielectric lens in this case would be half that of the conventional one and that such a reflector-lens could be used as an alternative to a conventional parabolic reflector. An experimental demonstration of this antenna will be reported in a future publication. Although this antenna is thinner than the above-mentioned antennas, the techniques make further reduction possible without affecting the performance. A variable-length dielectric-loaded planar reflector and a non-uniform dielectric thickness-profiled reflectarray are reported in [7, 8], respectively. In [9], a reflector antenna loaded with a variable-thickness lens is reported for THz applications. The latter three studies employed a reflectarray design approach, which is extended here to realize a stepped lens-loaded flat reflector (STLR). In reflectarray design, the phase to be compensated at each position is estimated. The unit cell element is then designed and analysed by varying its geometrical parameter, to reflect the incident field with an appropriate phase such that a planar phase front is exhibited at the aperture [10]. Interpolation of the above-mentioned two steps leads to the realization of a reflectarray, which is discussed later in this paper [7–10]. By considering this study, a reduction in dielectric thickness is achieved compared to the SMLR [6], which in turn minimizes the dielectric losses and cost. As the unit cell approach is employed to achieve those attributes, the radiation pattern of the proposed antenna is also compared with that of the resonant microstrip reflectarray.

Received 9 April 2019, Accepted 5 June 2019, Scheduled 19 June 2019

* Corresponding author: Krishnasamy T. Selvan (selvankt@ssn.edu.in).

[1] Department of Electronics and Communication Engineering SSN College of Engineering, Kalavakkam, India. [2] SAMEER-Center for Electromagnetics, Taramani, Chennai, India.

Teflon is the material chosen for the study, and all the simulations are carried out with CST Microwave Studio (CST MS) 2017.

The reflection-phase performance of the flat reflector backed dielectric unit cell is estimated in Section 2. Subsequently, design and analysis of the STLR antenna using this element are described in Section 3. A study on the effect of tapering of the stepped structure is also included. In Section 4, the simulated and experimental results of the proposed antenna are given. Also, a comparison of the proposed antenna with an SMLR and a microstrip reflectarray is presented. Section 5 summarizes the key results of the work.

2. THE REFLECTION-PHASE PERFORMANCE OF THE UNIT CELL

2.1. Unit Cell Design

The major steps in the reflectarray design are the estimation of the compensation phase and element analysis. The phase distribution is calculated using the following simple parabolic equation [8].

$$\text{Compensation phase, } \varphi_{mn} = k_0 \left(R_{mn} + \vec{r}_{mn} \cdot \vec{u}_0\right) + 2p\pi, \quad \text{in degrees, } p = 0, \pm 1, \pm 2, \ldots \tag{1}$$

where k_0 $(= \pi\lambda_0)$ is a free space propagation constant; R_{mn} is the spatial distance between the focal point and the mnth element; $\vec{r}_{mn}$ is the position vector of the element; and $\vec{u}_0$ indicates the desired beam direction vector.

A metal-backed dielectric unit cell element of size $0.5\lambda_0 \times 0.5\lambda_0$ is then designed at 10 GHz, where λ_0 is the free space wavelength. Its reflection phase performance is simulated by employing the infinite array (unit cell) approach using CST MS as shown in Fig. 1(a).

2.2. Theoretical Estimation of the Reflection Phase

While the simulation tool is largely utilized for the estimation of the reflection phase, the theoretical approach is always of interest to the research community [11]. The following equation is adopted from [8] to estimate the reflection phase of the metal-backed dielectric unit cell, where it has been derived using transmission line model with the help of ABCD parameters.

$$\text{Reflection phase} = -2\tan\left(\frac{Z_c}{Z_s}\tan\left(\beta t_d\right)\right), \text{ in degrees} \tag{2}$$

where t_d is the dielectric thickness; Z_c, β, and Z_s are the characteristic impedance, propagation constant, and surface impedance, respectively, and are calculated using Eqs. (6), (7), and (10) in [8], respectively.

The reflection phase of the proposed unit cell is calculated using Eq. (2) at 10 GHz for various dielectric thicknesses. It is then compared with the simulated reflection phase performance, and a good match is noted between them as evidenced in Fig. 1(b).

2.3. Reflection Phase Bandwidth of the Element

To estimate the phase bandwidth of the unit cell element, simulated reflection phase performances are estimated at 8 GHz and 12 GHz. They are plotted as a function of lens thickness in Fig. 1(b). It is observed that the estimated reflection phases at the three frequencies are parallel to each other, with an acceptable phase deviation of $\pm 45^\circ$ with respect to the centre frequency [12]. Consequently, the unit cell element offers a wider phase bandwidth about 40%.

2.4. Effect of Excitation Mode and Incident Angle on the Element's Reflection Phase

The unit cell is analysed for the reflection phase performance by exciting the input port with two fundamental modes, TE_{00} and TM_{00}. An excellent match is noted as shown in Fig. 1(b), which indicates that it can be used for a dual polarized operation. To see the effect of incident angles on the reflection phase of the element, the reflection phase is estimated for various θ and ϕ values, which are then plotted as a function of lens thickness in Fig. 1(c). It is observed that for a given lens thickness, the variation in the reflection phase is less than 45° for all the cases. Therefore, this element can be used to construct

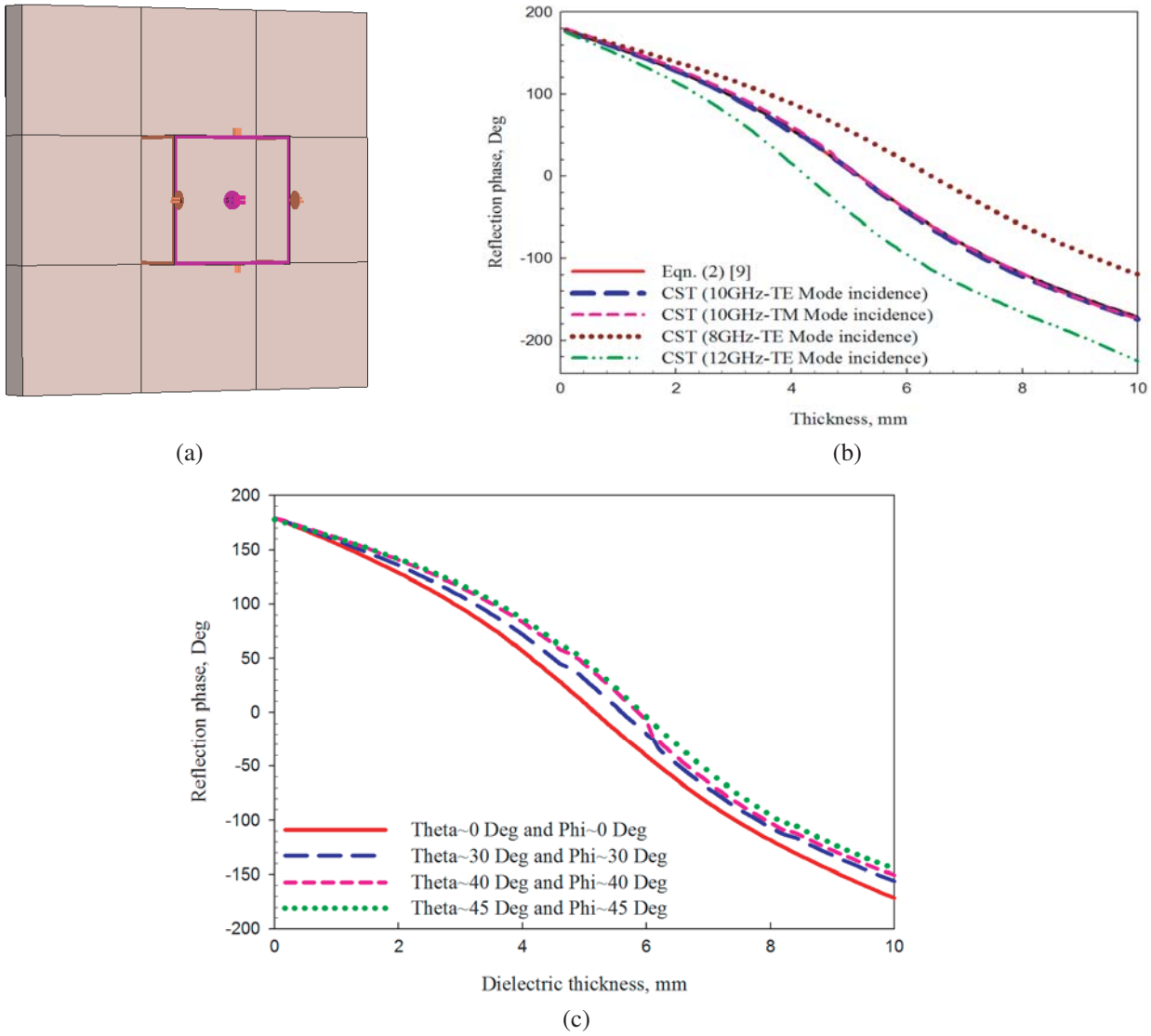

Figure 1. Reflection phase performance of the metal backed dielectric, (a) unit cell simulation model, (b) theory and CST MS at 10 GHz, and using CST MS at 8 GHz and 12 GHz, and (c) for various incident angles at 10 GHz.

a large-sized antenna and also for offset feed configurations, where the maximum incident angle of the feed illumination to the element is about $\pm 45°$.

2.5. Comparison of the Reflection Phase Behaviour of the Dielectric Element and a Resonant Patch

To show the reflection phase bandwidth behaviour of narrow and wideband elements, a comparison of the reflection phase performances of the unit cell and of a simple, variable size microstrip patch element is presented in Fig. 2. It is evident that the reflection phase of the patch is highly sensitive near resonance, whereas the metal backed dielectric unit cell offers a smooth phase response as anticipated, due to its wideband nature [12, 13]. The effect of this characteristic of the element on an antenna system performance is described in Section 4.4 of this paper.

Next, elements with an appropriate thickness are placed in accordance with the compensating phase over a ground plane, whose analysis is described in the next section.

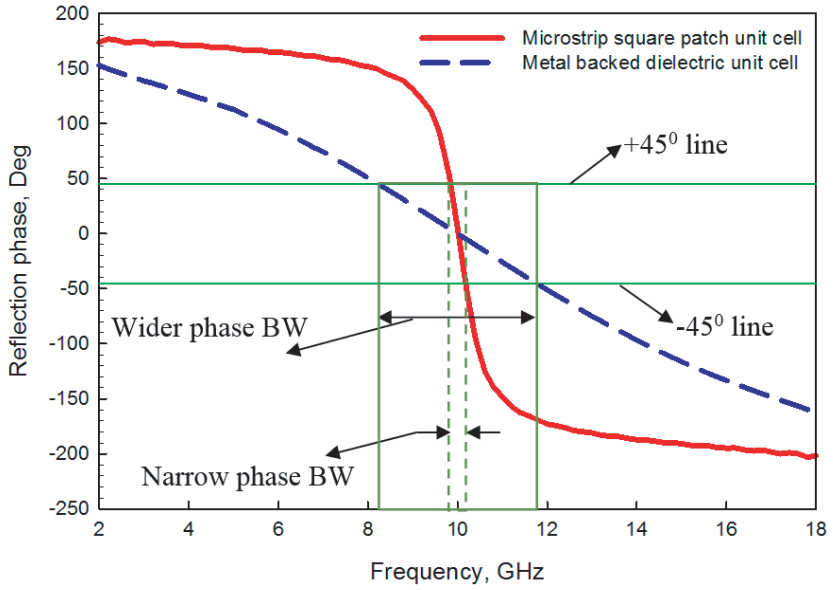

Figure 2. Phase bandwidth performance of the proposed unit cell and a variable size resonant patch.

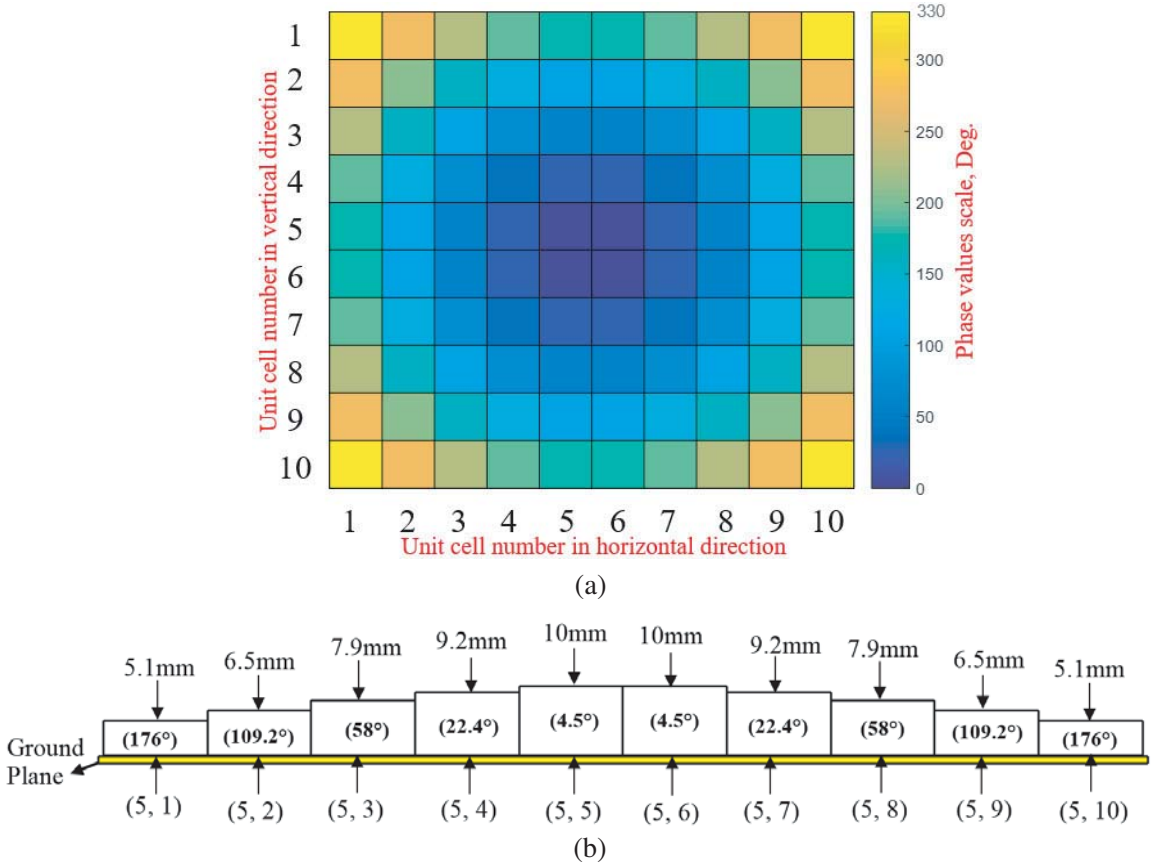

Figure 3. (a) Phase distribution as a function of position at $f_0 = 10\,\text{GHz}$ and (b) element placement at each location according to the compensating phase in fifth row.

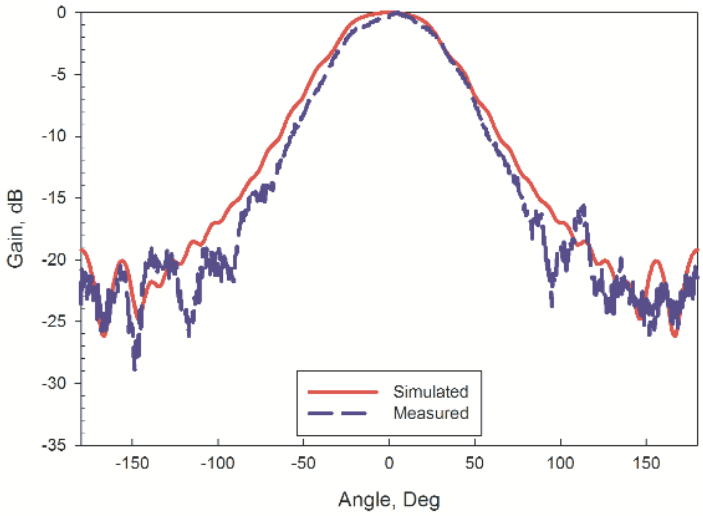

Figure 4. Simulated and measured radiation patterns of the feed horn in the H-plane at 10 GHz.

3. DESIGN AND ANALYSIS OF STEPPED DIELECTRIC LENS-LOADED PLANAR REFLECTOR

3.1. STLR Antenna Design

The plane reflector of size $5\lambda_0 \times 5\lambda_0$ (15 cm × 15 cm) is considered. And the phase that needs to be compensated at each position of that reflector is estimated using Eq. (1) at 10 GHz, for the feed location of (0, 0, 15 cm) and beam direction of ($\theta_b = 0°$ and $\phi_b = 0°$), as shown in Fig. 3(a). Unit cell elements are then placed appropriately in accordance with the compensation phase at each location by interpolating the data presented in Figs. 1(b) and 3(a). For example, the placement of a dielectric element of varied thickness according to the phase distribution for a one-dimensional (fifth row of Fig. 3(a)) case is shown in Fig. 3(b). Likewise, the whole reflector is loaded with an array of 10 × 10 elements (dielectric unit cell) to compensate the phase values calculated above and thus achieve a planar phase front. The STLR is examined by employing an available rectangular pyramidal horn as the centre feed. The aperture size of this horn is 2.75 cm × 2 cm, and its simulated and measured radiation patterns are plotted in Fig. 4. Moreover, the horn offers a typical gain of 9 dB at 10 GHz and a feed taper of about 2 dB at the edge of the reflector, which is calculated from the measured pattern.

3.2. STLR Antenna Analysis

The reflector-stepped lens configuration is depicted in Fig. 5(a), which is then analyzed with a feed horn using transient solver of CST MS simulation tool as shown in Fig. 5(b). To examine the effect of tapering of the stepped dielectric structure, two such designs are realized as shown in Fig. 5(c). The simulated performance of the reflector with these structures has shown a similar performance to that of the one with the stepped dielectric lens. Furthermore, the design of the proposed antenna involves a simple reflectarray unit cell approach along with the concept of the lens (varying dielectric thickness for phase compensation), which results in an easy realization of high gain antennas. The STLR antenna is evaluated through simulation and experiment for its radiation performances, which are presented in the next section.

4. PERFORMANCE EVALUATION

4.1. Numerical and Experimental Results

The STLR along with a feed horn is examined for its radiation pattern and gains by simulation, where optimal performance is obtained at a focal distance (F) of 19.8 cm. Subsequently, the stepped

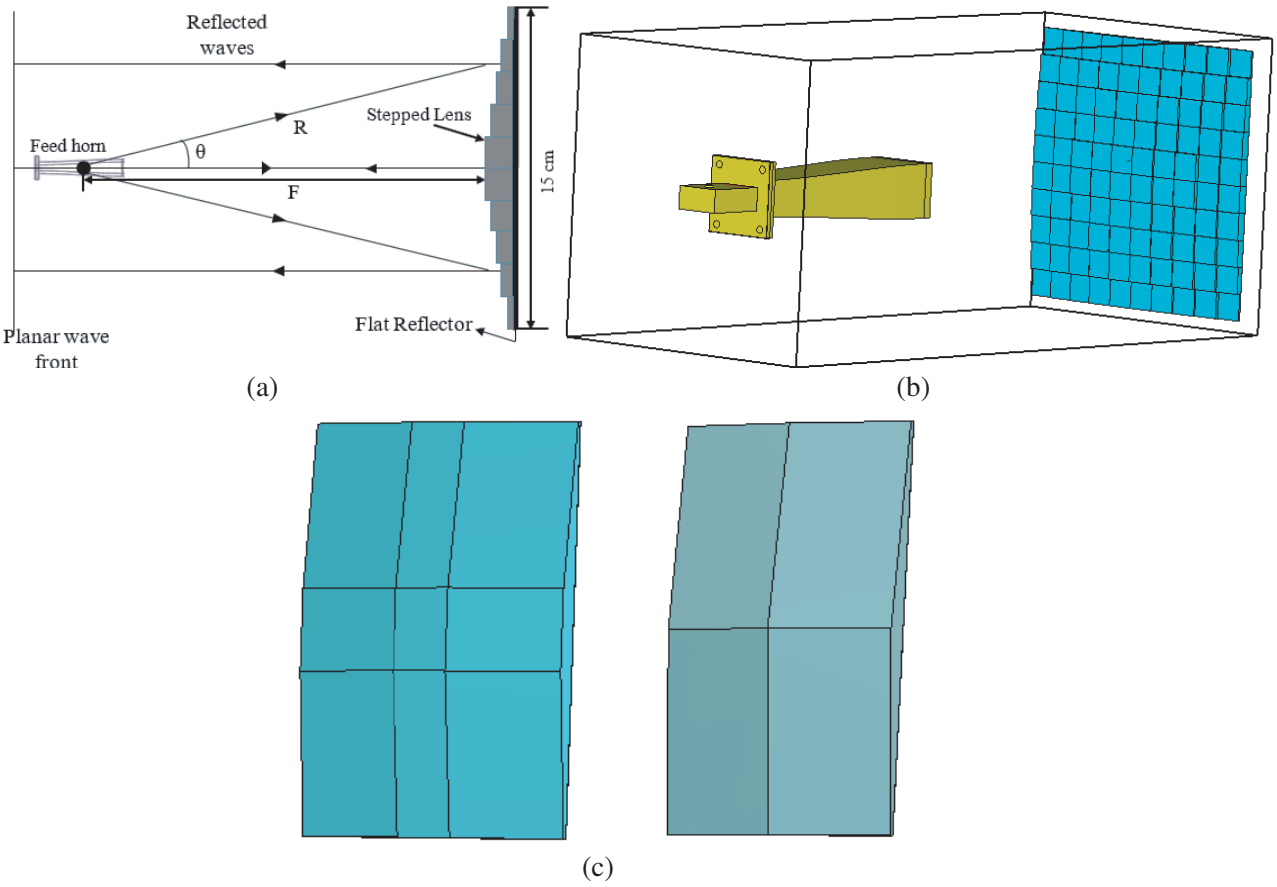

Figure 5. (a) STLR configuration and simulation models of planar reflector loaded with (b) stepped dielectric lens and (c) tapered dielectric slab.

dielectric lens is fabricated using CNC milling machine, and its prototype is shown in Fig. 6. It is evaluated for radiation patterns in a far-field experimental setup at the open terrace, SAMEER-Center for Electromagnetics, Chennai. In this measurement, the AUT was mounted at the height of 2.5 m, and it was placed at a distance of 4.5 m from the transmitting pyramidal horn antenna. The radiation patterns are estimated in the H-plane alone, due to the limited time for which the authors had access to the measurement facility. Here the optimized focal distance is found to be 18.5 cm. The simulated and measured radiation patterns are compared at the two edges and centre frequencies (8, 10, and 12 GHz) of X-band in the H-plane, which is displayed in Figs. 7(a)–(c). A fair match is noted between them at all considered frequencies. The measured 3-dB beamwidth values of 12°, 9°, and 7°, and side-lobe levels of −10 dB, −8.6 dB, and −7.9 dB are noted at 8, 10, and 12 GHz, respectively. To see how the STLR performance compares with that of an SMLR, a simulation-based study is carried out, as described next.

4.2. Performance Comparison with an SMLR

To see how the radiation performance of the STLR antenna compares with its rival, an SMLR antenna of an equivalent cross section is considered, whose configuration is shown in Fig. 8(a). Here the lens is designed by calculating the slant length R using Eq. (3) at 10 GHz, for a focal distance (F) of 15 cm [6].

$$R = \frac{(n-1)\,2F}{(2n-1)\cos\theta - 1} \tag{3}$$

Here, the lens was initially designed with a circular aperture of 10.6 cm radius and then appropriately sliced to realize a square aperture as shown in Fig. 8(b). It is of interest to note that the maximum

Figure 6. Fabricated prototype of STLR.

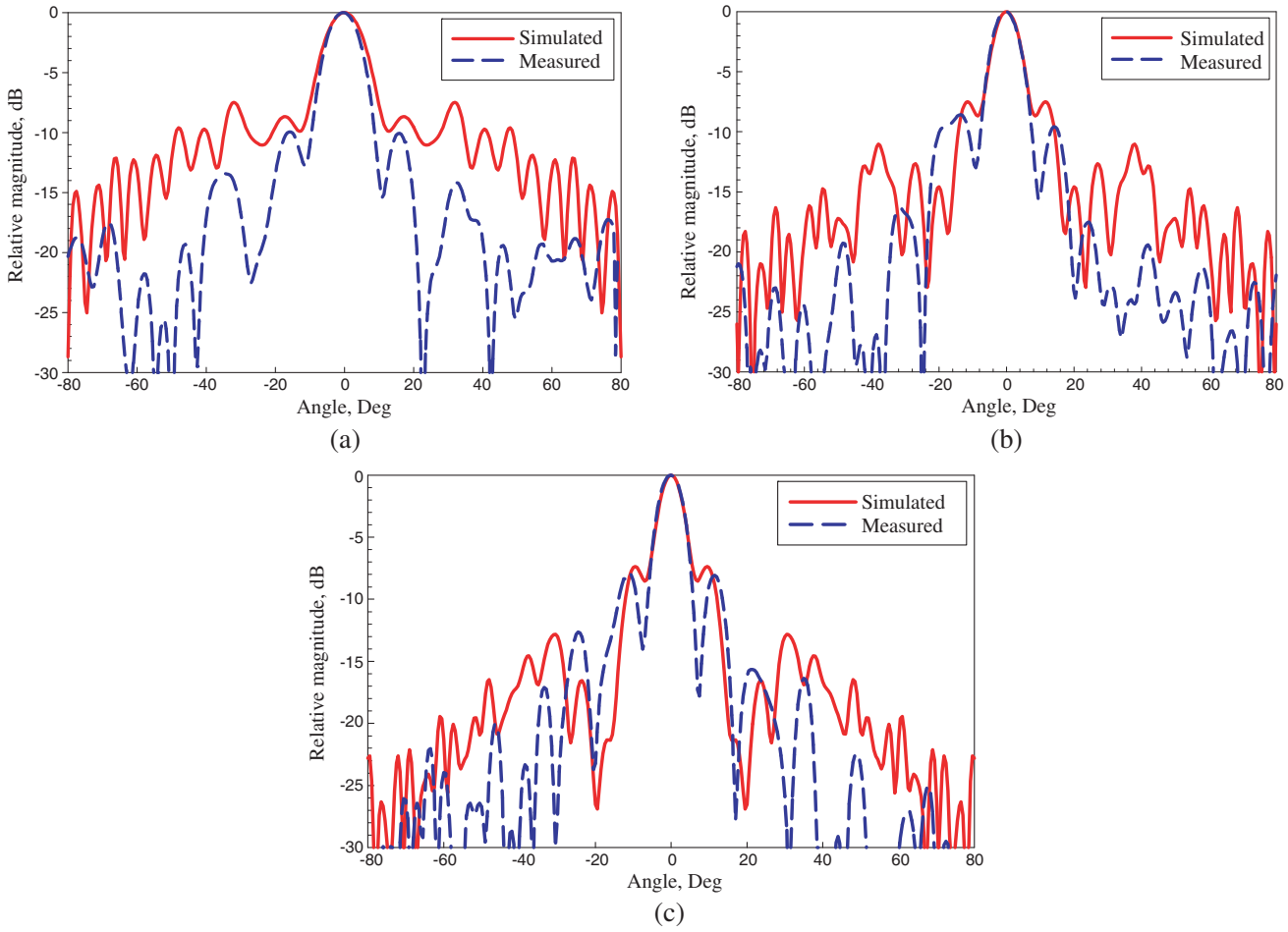

Figure 7. Simulated and measured radiation pattern of the STLR in the H-plane at (a) 8 GHz, (b) 10 GHz, and (c) 12 GHz.

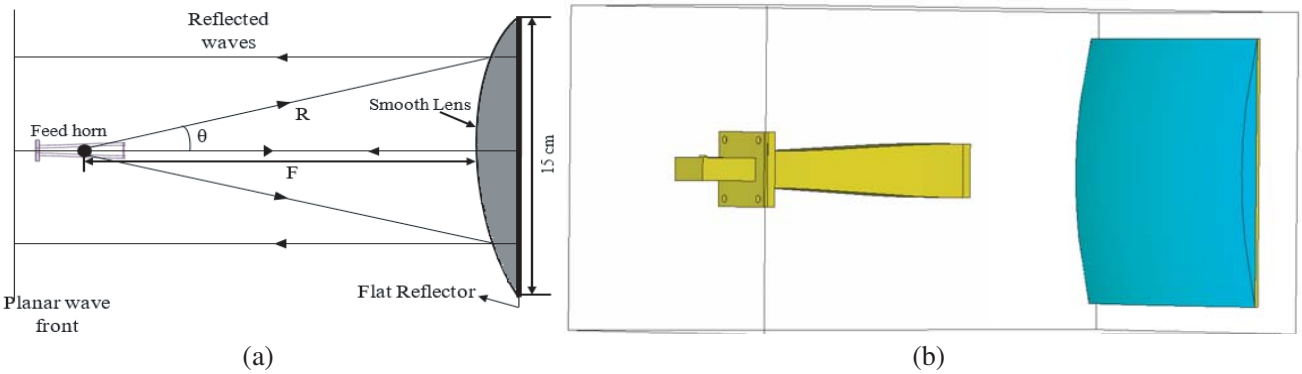

Figure 8. Planar convex smooth dielectric lens loaded flat reflector, (a) configuration and (b) simulation model.

thickness of the stepped lens is half that of the reflector-lens proposed by Kraus [6]. Thus, the proposed dielectric lens is thinner, light in weight, and thus will have much lower dielectric losses and fabrication cost. The SMLR along with the above-mentioned feed horn is examined for radiation performance with the help of a simulation tool as shown in Fig. 8(b). The optimum performance is achieved for a focal distance of 14.3 cm. The E- and H-plane radiation patterns of the two structures are shown in Figs. 9(a)–(c), at 8, 10, and 12 GHz, respectively. The STLR antenna performs as well as the SMLR. Additionally, the gains of those antennas are also estimated by using simulation software in X-band frequencies in steps of 0.2 GHz. They are then plotted as a function of frequency in Fig. 10(a), and a fair match is noted. The aperture efficiency values of the STLR and SMLR are plotted as a function of frequency in Fig. 10(b), and considerable agreement is observed. A maximum aperture efficiency of 32% and 35% is noted for STLR and SMLR, respectively. This small deviation is believed to be caused by the discretized phase compensation and diffractions at the edges of dielectric unit cells, in the case of STLR [4]. Interestingly, the gain and aperture efficiency behaviour of both antennas are similar to that of an aperture antenna, that is, those gain values monotonically increase as a function of frequency. As the STLR offers fairly comparable performance with that of SMLR, the proposed approach could be used as an alternative method to realize light weight and low loss metal-backed lenses. Furthermore, from these studies, which are carried out as an academic interest, it is inferred that the STLR has the potential for use in wideband applications as it is simple to design and realize.

Further, the gain performance at centre and edge frequencies, and bandwidth performance of the STLR and SMLR antennas are compared in Table 1. The proposed antenna offers a comparable gain and 3-dB gain bandwidth performances with that of the SMLR but with half the lens thickness as shown in Table 1 and Fig. 10.

Table 1. Performance comparison of the STLR and SMLR antennas in X-band.

Parameter		**Performance comparison**	
		STLR	**SMLR**
Gain, dB	8 GHz	14.7	16.3
	10 GHz	19.2	19.9
	12 GHz	21.6	21.9
3-dB gain bandwidth		22.3%	22.3%
Maximum thickness of the lens		1 cm	2 cm

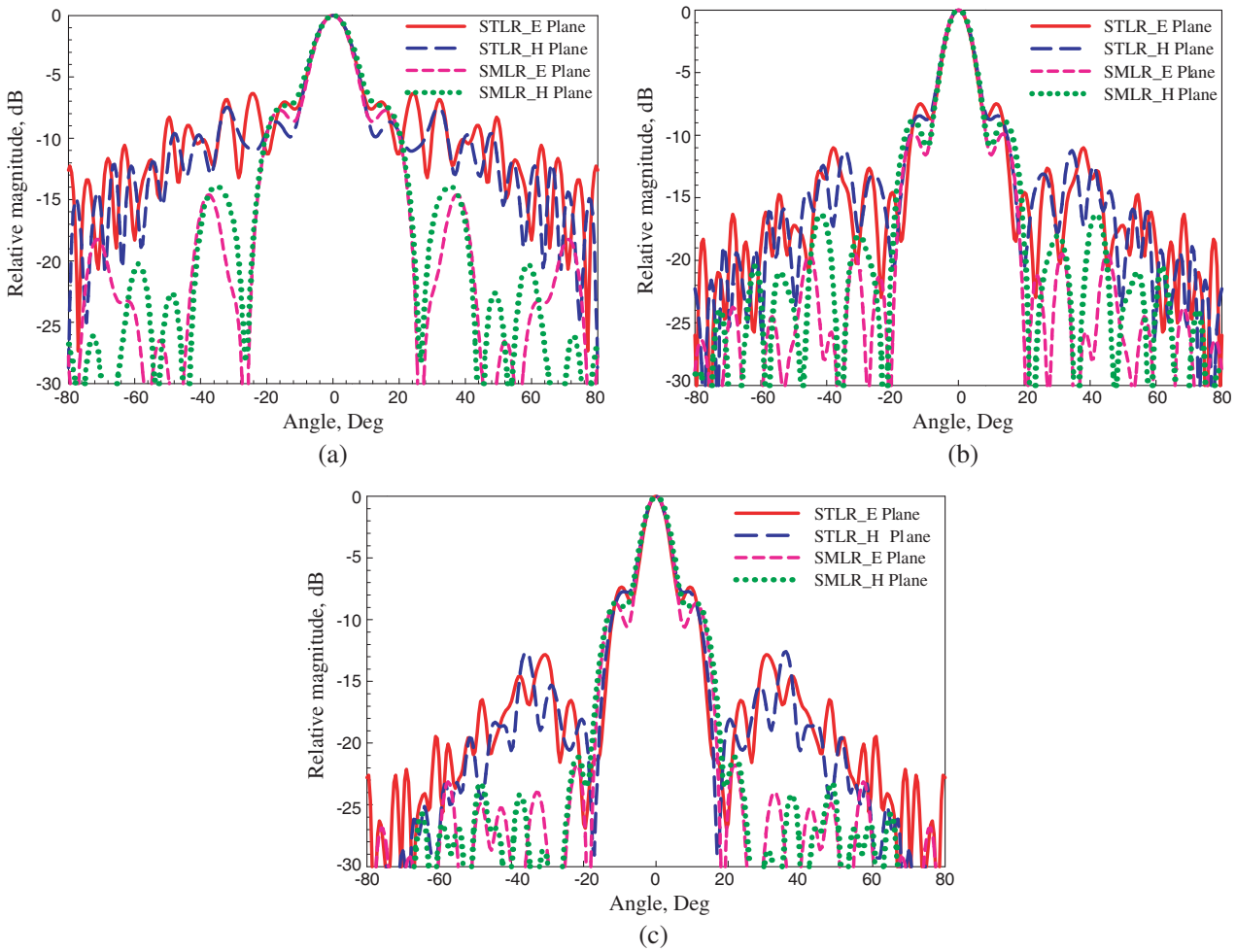

Figure 9. Simulated radiation pattern of the STLR and SMLR antennas in both E and H planes for (a) 8 GHz, (b) 10 GHz, and (c) 12 GHz.

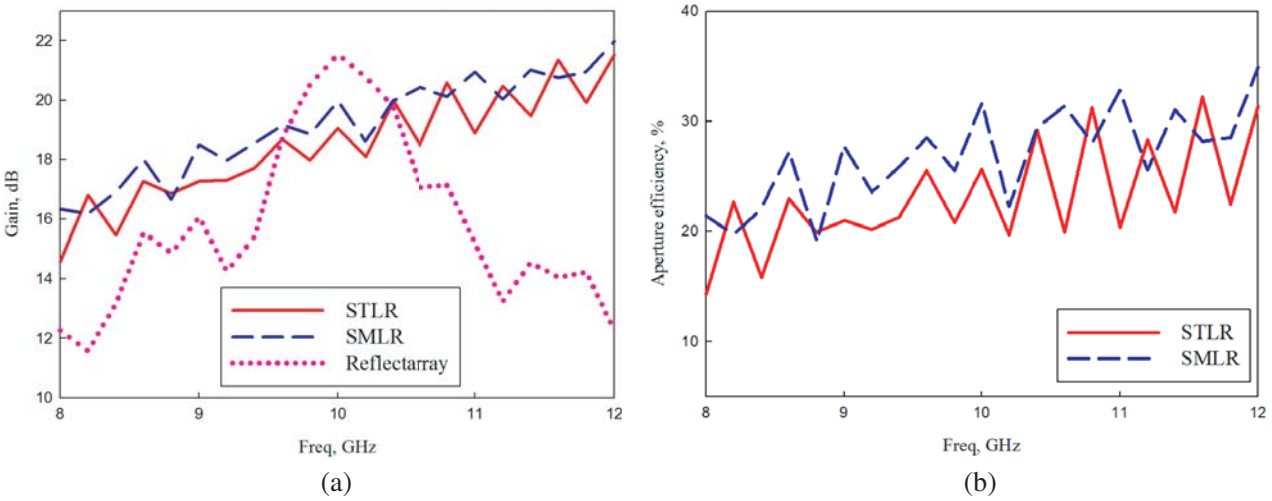

Figure 10. (a) Gain performances of the STLR, SMLR, and resonant microstrip reflectarray antennas and (b) aperture efficiency values of STLR and SMLR, as a function of frequency.

4.3. Application of the Proposed Design Approach in Shaped Beam Antenna Design

In contour beam applications, the shaping of the lens is very difficult for an SMLR antenna due to various constraints as observed for a parabolic reflector [14]. While the operation of a shaped parabolic reflector is easily accomplished by the reflectarray, an alternate design method for conductor-backed dielectric lens in such applications would be of great research interest. From the above studies, we note that the STLR antenna performs as well as an SMLR antenna. Therefore, to realize a shaped beam reflector lens, the phase distribution needs to be estimated for a given beam shape, then appropriate dielectric unit cell elements are placed as done in contour beam reflectarray [15]. Therefore, the STLR antenna can be a good and simple alternative design methodology for realizing conductor-backed lenses to exhibit a specific beam pattern.

4.4. Performance Comparison with the Microstrip Reflectarray

The STLR antenna is realized by employing a reflectarray design procedure. Hence, it would be of interest to compare the radiation pattern of the proposed antenna with that of a microstrip reflectarray. To facilitate this, a resonant reflectarray of equivalent cross section is designed with variable size patch elements at 10 GHz. It is then analysed with the above-mentioned feed horn by using a simulation tool. The estimated E- and H-plane radiation patterns are then compared with the one obtained for the proposed antenna at 10 GHz, which are displayed in Fig. 11. A good agreement is noted between pattern main lobes of both structures; however, the side lobe level of the STLR antenna is larger than that of the reflectarray. Additionally, the gains of reflectarray are plotted as a function of frequency (dotted line) in Fig. 10. It is observed that the microstrip reflectarray offers about 2 dB higher gain than that of the proposed one. The gain drop and larger side lobe level of the STLR antenna are believed to be caused by its wideband nature and dielectric losses associated with the lens [13].

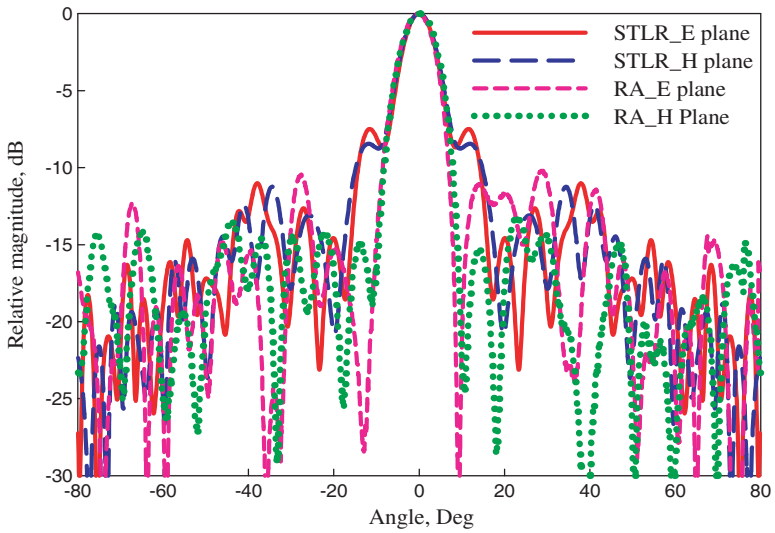

Figure 11. Simulated radiation patterns of the STLR and resonant microstrip reflectarray, at 10 GHz.

5. CONCLUSION

A flat reflector loaded with a stepped dielectric lens was designed and analysed by employing a reflectarray unit cell design procedure, in X-band. It was fabricated and then measured for gain and radiation pattern performances. Simulated and experimental results exhibited a good correlation over the whole frequency band. Subsequently, the radiation pattern and gain performances of the proposed antenna were compared with that of a planar reflector antenna loaded with the smooth lens, and it was found to be analogous. Furthermore, the thickness of the stepped lens was almost half that of the SMLR. The gain and radiation pattern performances were also compared with that of the resonant

microstrip reflectarray at the design frequency. A relatively less gain and high side lobe values were noted for the STLR, which is believed to be due to a wideband nature of the proposed one.

ACKNOWLEDGMENT

This work was supported in part by the Indian Space Research Organization Sponsored Research programme (ISRO-RESPOND) under the grant ISRO/RES/3/728/16-17. The authors would like to thank Mr. M. Srinivasan and Mr. I. Balakrishna of SAMEER-Center for Electromagnetics, Chennai for their support during measurement.

REFERENCES

1. Pozar, D. M., S. D. Targonski, and H. D. Syrigos, "Design of millimeter wave microstrip reflectarray," *IEEE Transactions on Antennas Propagation*, Vol. 45, No. 2, 286–295, February 1997.
2. Huang, M., S. Yang, W. Xiong, and Z. Nie, "Design and optimization of spherical lens antennas including practical feed models," *Progress In Electromagnetics Research*, Vol. 120, 355–370, 2011.
3. Barry, D. G., R. Malech, and W. Kennedy, "The reflectarray antenna," *IEEE Transactions on Antennas and Propagation*, Vol. 11, 645–651, November 1963.
4. Shafai, L., "Dielectric loaded antennas," *Encyclopedia of RF and Microwave Engineering*, John Wiley & Sons, April 2005.
5. Jain, S. and R. Mittra, *Computational Electromagnetics: Chapter 15 — Field Transformation Approach to Designing Lenses*, 539–552, Springer, New York, June 2013.
6. Kraus, J., "Some unique reflector-type antennas," *IEEE Antennas and Propagation Society Newsletter*, Vol. 24, No. 2, 9–12, April 1982.
7. Zainud-Deen, S. H., N. Ahmed, H. A. El-Azem Malhat, S. Gaber, and K. H. Awadalla, "Dielectric resonator antenna reflectarrays mounted on or embedded in conformal surfaces," *Progress In Electromagnetics Research C*, Vol. 38, 115–128, 2013.
8. Moeini-Fard, M. and M. Khalaj-Amirhosseini, "Nonuniform reflect-array antennas," *International Journal of RF and Microwave Computer-Aided Engineering*, Vol. 22, No. 5, 1–6, August 2011.
9. Deng, R., L. Matekovits, F. Yang, P. Pirinoli, S. Xu, and M. Li, "Design of a flexible dielectric reflectarray antenna for THz applications," *Proceedings of 9th European Conference on Antennas and Propagation (EuCAP), 2015*, Lisbon, Portugal, April 2015.
10. Ng, W.-H., E. H. Lim, F.-L. Lo, and K.-H. Tan, "Double-layered circular microstrip reflectarray element with broad phase range," *Progress In Electromagnetics Research C*, Vol. 50, 155–164, 2014.
11. Lingasamy, V., K. T. Selvan, and S. Rengarajan, "On the reflection phase characteristics of rectangular and circular patch reflectarray elements," *Proceedings of Antennas and Propagation International Symposium (APSYM) 2016*, CUSAT, Cochin, December 2016.
12. Bozzi, M., S. Germani, and L. Perregrini, "Performance comparison of different element shapes used in printed reflectarrays," *IEEE Antennas and Wireless Propagation Letters*, Vol. 2, 219–222, August 2003.
13. Guha, D. and C. Kumar, "Microstrip patch versus dielectric resonator antenna bearing all commonly used feeds: An experimental study to choose right element," *IEEE Antennas and Propagation Magazine*, Vol. 58, No. 1, 45–55, February 2016.
14. Fernandes, C. A., "Shaped dielectric lenses for wireless millimeter-wave communications," *IEEE Antennas and Propagation Magazine*, Vol. 41, No. 5, 141–150, October 1999.
15. Capozzoli, A., C. Curcio, A. Liseno, and G. Toso, "Fast, phase-only synthesis of aperiodic reflectarrays using NUFFTs and CUDA," *Progress In Electromagnetics Research*, Vol. 156, 83–103, 2016.